



## OPEN ACCESS

## EDITED BY

Ben-Xin Wang,  
Jiangnan University, China

## REVIEWED BY

Sandeep Dahiya,  
Bhagat Phool Singh Mahila  
Vishwavidyalaya, India  
Giuseppe Brunetti,  
Politecnico di Bari, Italy

## \*CORRESPONDENCE

Qiuhui Chu,  
✉ chuqiuhui@163.com

RECEIVED 15 April 2025

ACCEPTED 12 June 2025

PUBLISHED 02 July 2025

## CITATION

Shu Q, Zhang C, Li F, Chu Q, Guo C, Li F,  
Zhang H, Tao R, Lin H and Wang J (2025)  
Impact of mode instability on polarization  
extinction ratio in backward pumped fiber  
amplifiers.  
*Front. Phys.* 13:1612074.  
doi: 10.3389/fphy.2025.1612074

## COPYRIGHT

© 2025 Shu, Zhang, Li, Chu, Guo, Li, Zhang,  
Tao, Lin and Wang. This is an open-access  
article distributed under the terms of the  
[Creative Commons Attribution License \(CC  
BY\)](https://creativecommons.org/licenses/by/4.0/). The use, distribution or reproduction in  
other forums is permitted, provided the  
original author(s) and the copyright owner(s)  
are credited and that the original publication  
in this journal is cited, in accordance with  
accepted academic practice. No use,  
distribution or reproduction is permitted  
which does not comply with these terms.

# Impact of mode instability on polarization extinction ratio in backward pumped fiber amplifiers

Qiang Shu, Chun Zhang, Fang Li, Qiuhui Chu\*, Chao Guo, Fengyun Li, Haoyu Zhang, Rumao Tao, Honghuan Lin and Jianjun Wang

Research Center of Laser Fusion, China Academy of Engineering Physics, Mianyang, China

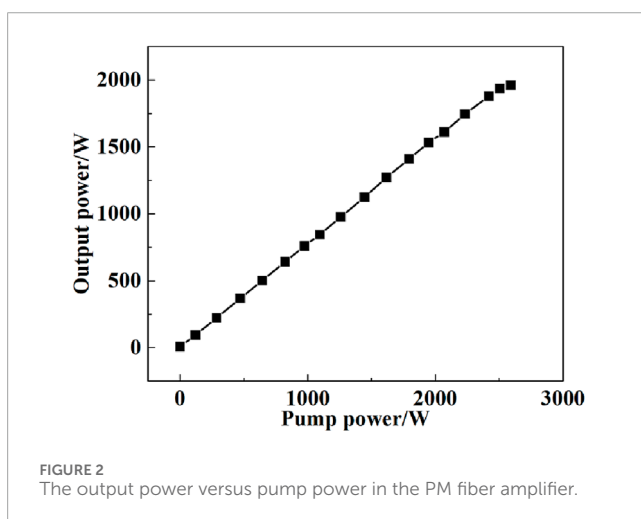
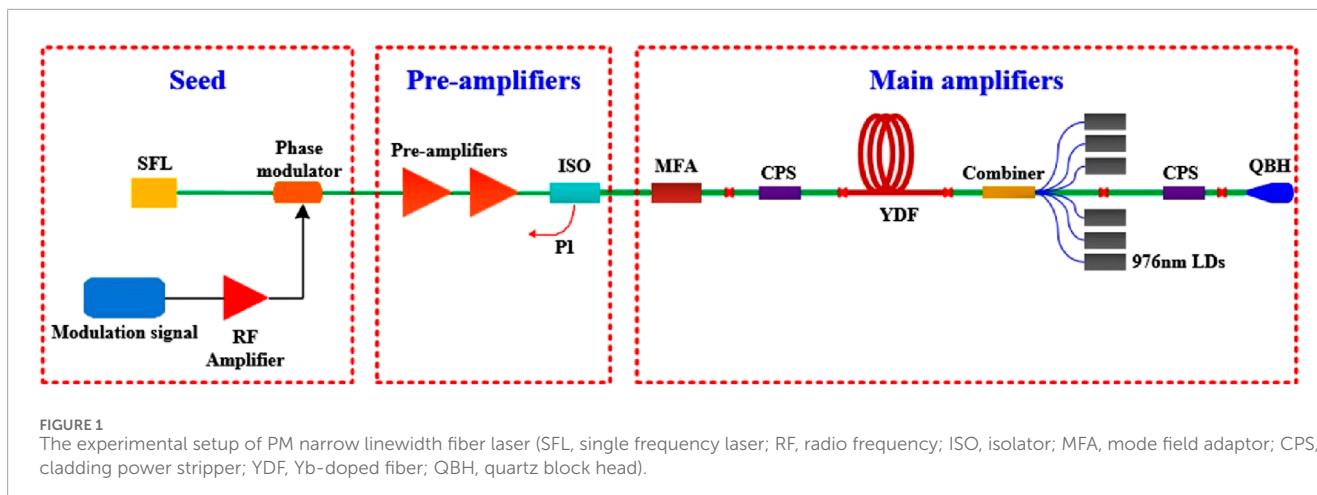
The influence of mode instability (MI) on polarization extinction ratio (PER) has been investigated in a 2 kW level polarization-maintained (PM) fiber laser system with backward pumping configuration, and the phenomena is different from the existing observations in forward-pumped PM fiber amplifiers. No decrease in PER was noted with the onset of MI, revealing that the MI effect has little impact on PER in backward-pumped PM fiber amplifiers. The discrepancy induced by the pump configuration has been theoretically analyzed, which is attributed to the longitudinal-distribution difference of high order modes induced by the MI effect.

## KEYWORDS

mode instability, polarization extinction ratio, polarization-maintained fiber lasers, nonlinear effect, backward pump

## 1 Introduction

High power polarization-maintained (PM) fiber lasers with near-diffraction-limited beam quality have been widely used in many fields, such as gravitational wave detection [1], coherent radar system [2, 3], nonlinear frequency conversion [4–7], and coherent/spectral beam combining system [8–10]. For PM fiber lasers, beam quality and polarization extinction ratio (PER) are the key factors to evaluate laser performance, and attract great attention in the fiber laser society. Up to now, the output power of fiber lasers has been significantly improved, reaching a maximum level of 5 kW [11]. However, further power scaling of PM fiber lasers with great beam quality and PER are mainly limited by the nonlinear effects and the mode instability (MI) effect [12–15]. The MI effect originates from the thermal effect, which results in dynamic power coupling between the fundamental mode (FM) and high order modes (HOMs), and thereby dramatically deteriorates the beam quality and limits the output power. Even worse, recent experimental results in forward-pumped PM fiber lasers show that the MI effect can also result in a decrease in PER, which further limits the application of PM fiber lasers [16, 17]. However, the physical mechanism of MI induced degradation of PER in forward-pumped PM fiber laser has not been analyzed. On the other hand, the impact of MI on PER has only been reported in forward-pumped PM fiber lasers, and no related research in backward pumped configuration has been reported, to the best of



our knowledge [18–25]. Compared with the forward-pumped fiber lasers, the backward pumped ones have the advantages on suppressing the MI and nonlinear effects, and have been widely employed in high power PM fiber lasers [26–30], which deserve further investigation.

In this paper, a high power PM fiber amplifier has been established based on backward pumped master oscillator power amplifier (MOPA) structure. Based on the laser system, the influence of MI on PER has been investigated, and the results showed that the occurrence of MI in backward pumped PM fiber amplifier did not decrease PER, which is different from the results in forward pumped PM fiber amplifier. The physical mechanism has been discussed, and the simulation results illustrated that different pump power distributions can influence the leaking and reinjecting process of HOM, leading to the different results.

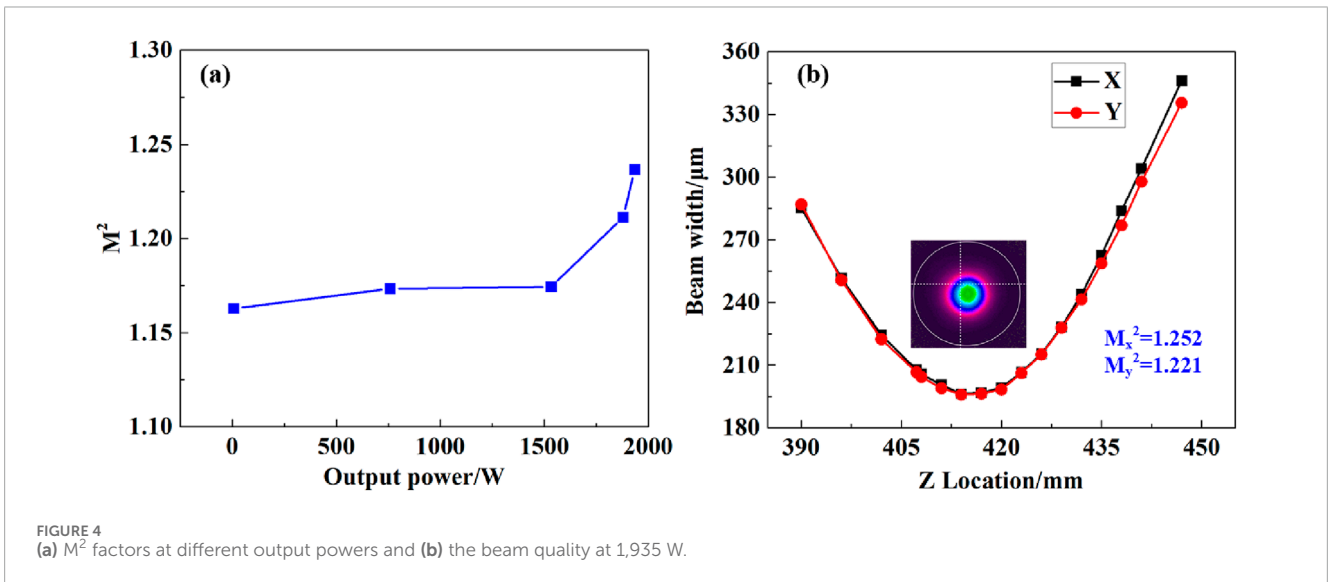
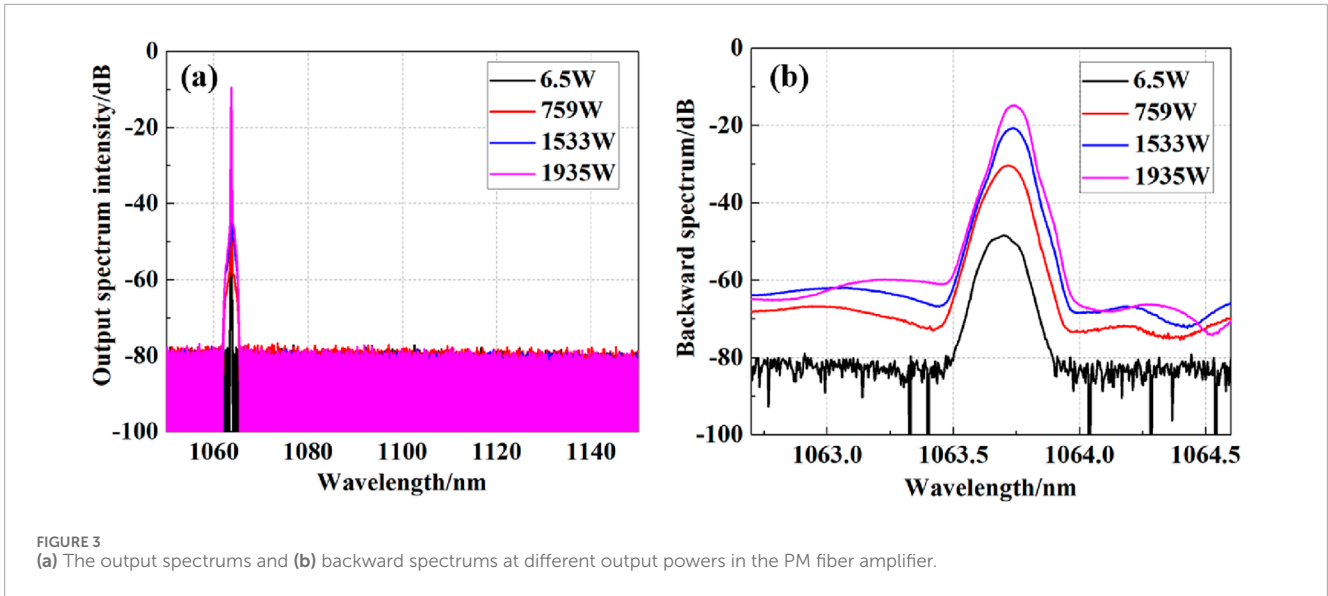
## 2 Experimental setup

The experimental setup of the MOPA system is shown in Figure 1. The seed was a single-frequency linear-polarized fiber laser with central wavelength being 1,064 nm and

spectrum linewidth being about 10 kHz, which delivers an output power of 20 mW. In order to suppress the stimulated Brillouin scattering effect (SBS), the spectrum linewidth of the seed laser was broadened to 0.2 nm by a phase modulator, which was driven by an amplified white noise signal (WNS). A filter was employed to adjust the frequency bandwidth of the WNS. The broadened seed laser was amplified by a three-stage all-fiber amplifier. Two pre-amplifiers boosted the laser power to about 20 W, where a PM Yb-doped fiber (YDF) with core diameter of 10  $\mu\text{m}$  and cladding diameter of 125  $\mu\text{m}$  was used. Then, the pre-amplified laser was injected into the main amplifier through a PM mode field adaptor (MFA). The 10/125  $\mu\text{m}$  YDF and MFA were used to ensure that the optical field injected into the main amplifier was near single-mode. Between the PM MFA and pre-amplifiers, a PM isolator (ISO) was inserted to prevent damage from backward light, and the multi-mode fiber port of ISO was used to monitor backward power and backward spectrum. The main amplifier was constructed by PM YDF with mode field diameter being 20  $\mu\text{m}$  and cladding diameter being 400  $\mu\text{m}$ , which was coiled tightly on a water-cooled aluminum plate to dissipate the heat and suppress MI. Six laser diode modules centered at 976 nm were coupled into the YDF through a (6 + 1)  $\times$  1 p.m. signal-pump combiner. By employing a 976 nm pump source to shorten the gain fiber length and utilizing 20/400  $\mu\text{m}$  PM YDF to enlarge the mode field area, the SBS effect was effectively suppressed. Two home-made PM cladding power strippers (CPSs) were used in main amplifier to strip the residual pump light and cladding signal light. A quartz block head was used to deliver the amplified laser, which was collimated by a collimator.

## 3 Experimental results

The output power was measured by the power meter, and the increase of output power versus pump power is shown in Figure 2. With the scaling of pump power, the output power of fiber laser increased linearly firstly. When the pump power was 2,419 W, the output power reached 1,880 W, and the optical-to-optical efficiency was about 78%. However, as the output power exceeded 1,880 W, the output power was barely growing with the



increasing of pump power, which indicated the efficiency decrease and the onset of MI [13].

An optical spectrum analyzer (OSA) with a resolution of 0.02 nm was used to record the output spectrum. The output spectrums at different output powers are shown in Figure 3a. The linewidth of seed laser was 0.2 nm, which remained constant and with output power scaling, and the SRS suppression ratio was higher than 70 dB at the maximum output power. The backward spectrums at different output powers are shown in Figure 3b. The backward spectrum manifested no sign of typical pulse, which confirmed that the laser system was free of SBS [31].

The beam quality factors  $M^2$  at different output powers were measured, and value of which were calculated by  $M^2 = \sqrt{((M_x^2)^2 + (M_y^2)^2)}/2$ . One can see from Figure 4 that, the  $M^2$  of the seed laser was 1.163 while it became 1.237 at the maximal output power of 1,935 W. When the output power was less than 1,880 W, the PM fiber laser kept near diffraction limited beam quality, and no

obvious degradation of beam quality was observed. However, when the output power exceeded 1,880 W, the beam quality degraded obviously, indicating the onset of MI [32].

It is well known that the MI effect can result in the beam quality distortion and the output efficiency decrease [32]. To further confirm that MI threshold was reached in the laser system, a photodiode (PD) with a hole of 1.0 mm diameter and bandwidth of 350 MHz was employed to sample the time fluctuations of the transverse beam profile, which has been widely used to monitor the MI effect [32–34]. The PD was placed on the center of the collimated beam to detect the temporal characteristic of beam profile fluctuations, which were monitored by an oscilloscope with bandwidth of 500 MHz. It should be mentioned that the hole of PD was smaller than the beam size, which excluded the impact of power fluctuation. The time-domain traces at different output power are shown in Figure 5a. One can see the output power remained stable at 1,745 W, while it fluctuated at 1,961 W. The time traces proved

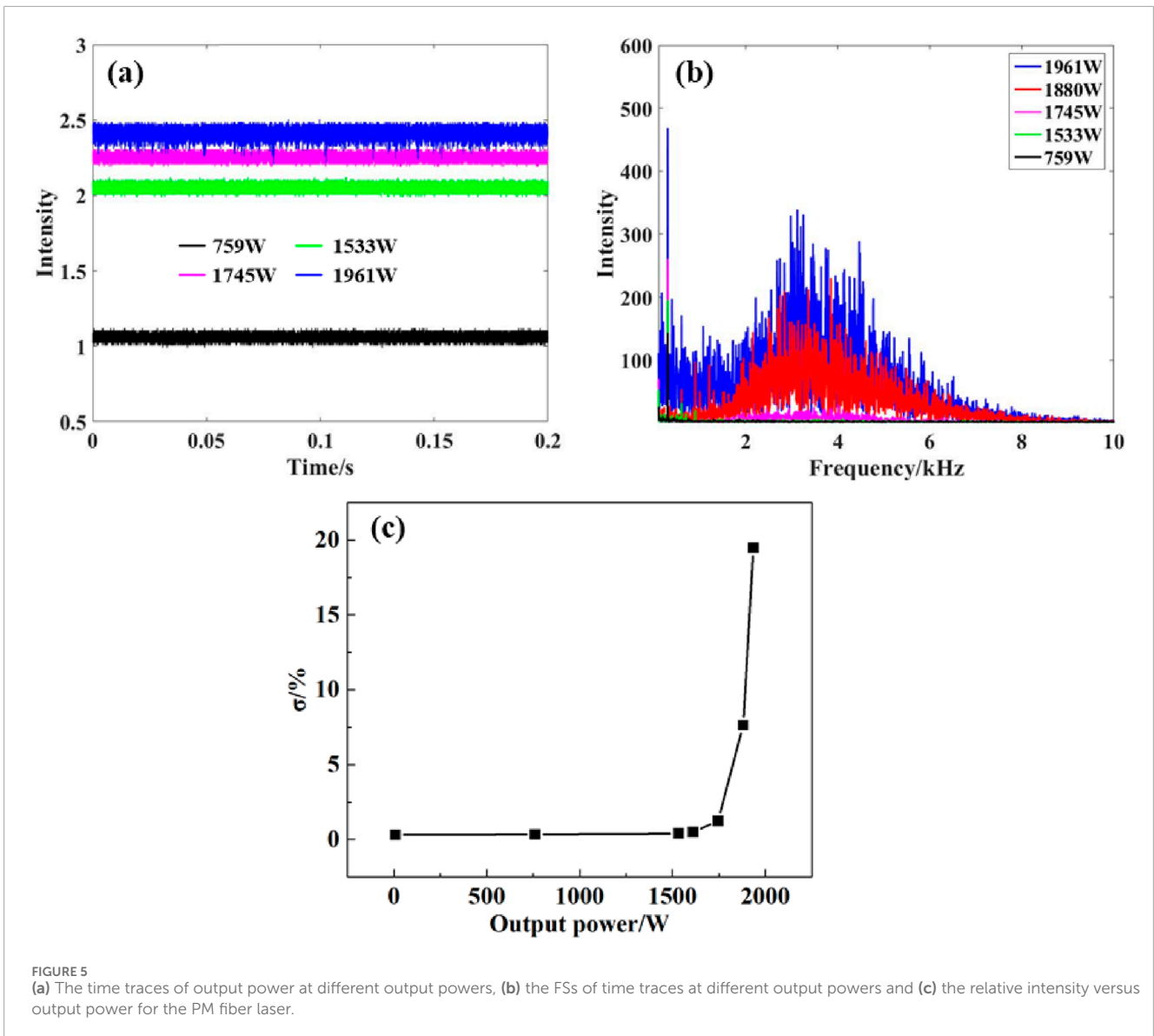


FIGURE 5 (a) The time traces of output power at different output powers, (b) the FSs of time traces at different output powers and (c) the relative intensity versus output power for the PM fiber laser.

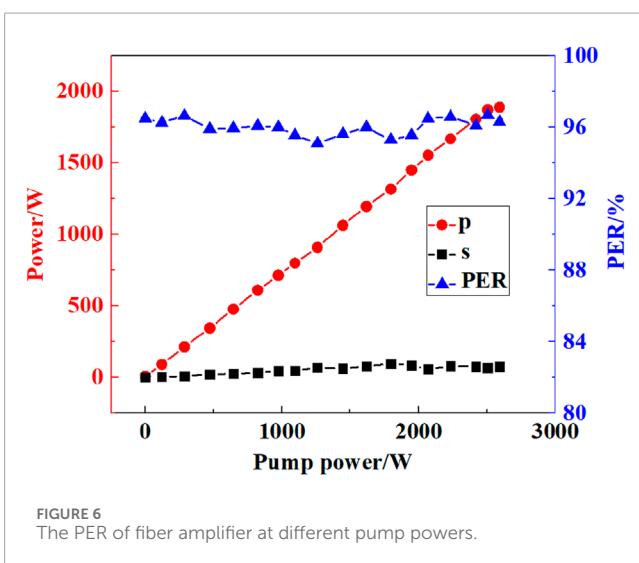


FIGURE 6 The PER of fiber amplifier at different pump powers.

that the onset of dynamic MI. Moreover, Fourier spectra (FSs) of the time traces at different output power levels were illustrated in Figure 5b. With the scaling of output power, obvious discrete noise lines appeared in the FSs, implying that the MI effect was onset. To quantitatively evaluate the MI effect, the relative intensity  $\sigma$  versus output power was inserted in Figure 5c, which was defined as  $\sigma = \int_0^{10\text{kHz}} P(\nu)d\nu / \int_{10\text{kHz}}^{20\text{kHz}} P(\nu)d\nu - 1$ , where  $P(\nu)$  was the power density at frequency of  $\nu$  [34]. Once the output power exceeds MI threshold, the frequency component will increase obviously in the range of 0–10 kHz, and  $\sigma$  will increase nonlinearly. Similar with Refs. [32, 34], the MI threshold was defined as the output power when  $\sigma$  reaches 5%. It can be concluded from Figure 5c that as the output power reached 1,880 W with  $\sigma$  being 7.63%, the relative intensity suddenly increased to 19% at 1,935 W, which suggested the MI threshold was 1,880 W [31, 33]. The evolution of relative intensity was similar with the results in Figure 2. After the onset of MI effect, large amount of HOMs will be generated and naturally decrease the beam quality. Furthermore, a part of the HOMs will leak into the fiber cladding

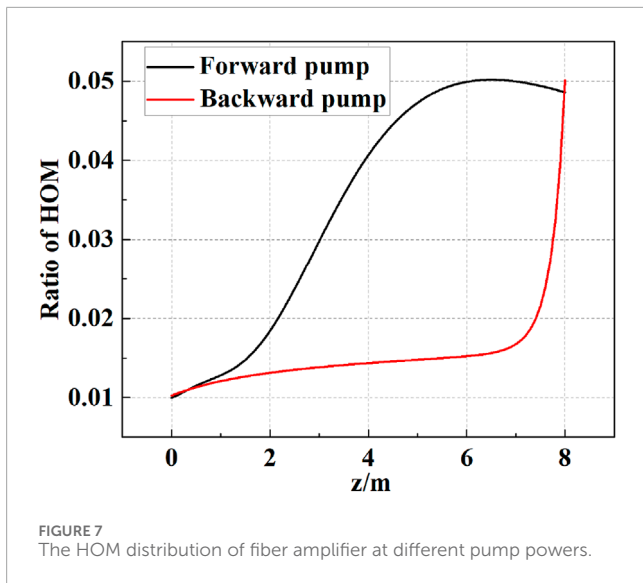


FIGURE 7 The HOM distribution of fiber amplifier at different pump powers.

due to fiber coiling, which will be stripped by CPS, resulting in the optical efficiency rollover shown in Figure 2.

The power of p-polarization light and s-polarization light and the PER at different pump powers are shown in Figure 6, which was measured by using assemble components of a half-wavelength plate and a polarization plate. With the increasing of the output power, the measured PER changed between 95.1% and 96.6% with about 1.5% of fluctuation, which was mainly induced by environmental noise and thermal noise. When the output power exceeded 1880 W, the MI occurred, but the PER did not decrease, and at maximum output power, the PER was 96.3% (14.32 dB), whereas for the forward-pump schemes, the PER dropped from over 94%–90% during MI occurrences [16], which indicates that the MI has little influence on PER of PM fiber laser with backward pumping configuration.

### 4 Discussion

The influence of the MI effect on PER of backward pumped PM fiber amplifier has been investigated in the experiment, and the results show that the MI effect has little impact. The phenomenon is different from the results in [16, 17], where the MI effect can result in the decrease of PER in the forward-pumped PM fiber amplifier.

The different relationships between MI and PER in PM fiber laser under different pump configurations may be attributed to the influence of the different pump power distributions [35]. In order to analyze the different results, the MI model is used to simulate the HOM distribution along the gain fiber, which can be expressed as

$$\begin{aligned} \xi(L) \approx & \xi_0 \exp \left[ \int_0^L dz \iint g(r, \phi, z) (\psi_2 \psi_2 - \psi_1 \psi_1) r dr d\phi \right] \\ & + \frac{\xi_0}{4} \sqrt{\frac{2\pi}{\int_0^L P_1(z) |\chi''(\Omega_0, z)| dz}} \\ & \exp \left\{ \int_0^L dz \iint g(r, \phi, z) (\psi_2 \psi_2 - \psi_1 \psi_1) r dr d\phi \right\} \\ & \times R_N(\Omega_0) \exp \left[ \int_0^L P_1(z) \chi(\Omega_0, z) dz \right] \end{aligned}$$

Where the  $\xi_0$  is the initial HOM fraction,  $L$  is the length of the gain fiber,  $\psi_i$  is the normalized electric field of fiber mode  $i$ , and  $P_1(z)$  is the power of fundamental mode.  $\chi(\Omega)$  is the nonlinear coupling coefficient, and  $\Omega_0$  represents the frequency of the maximum of  $\chi(\Omega)$ .  $\chi''(\Omega)$  denotes the second derivative of  $\chi(\Omega)$ .  $g(r, \phi, z)$  is the gain of the amplifier, which can be calculated by laser rate equation

$$\begin{aligned} \frac{N_2(r, \phi, z)}{N_1(r, \phi, z)} &= \frac{\frac{\sum P_p(z) \sigma_p^e \varphi_p(r, \phi)}{h\nu_p} + \frac{\sum P_s(z) \sigma_s^e \varphi_s(r, \phi)}{h\nu_s}}{\frac{\sum P_p(z) \sigma_p^e \varphi_p(r, \phi)}{h\nu_p} + \frac{\sum P_s(z) \sigma_s^e \varphi_s(r, \phi)}{h\nu_s} + \frac{1}{\tau}} \\ \pm \frac{dP_p^\pm(z)}{dz} &= \left\{ \int_0^{2\pi} \int_0^a [\sigma_p^e N_2(r, \phi, z) - \sigma_p^a N_1(r, \phi, z)] \varphi_p(r, \phi) r dr d\phi \right\} \\ &\quad \times P_p^\pm(z) - \alpha_p P_p^\pm(z) \\ \pm \frac{dP_s^\pm(z)}{dz} &= \left\{ \int_0^{2\pi} \int_0^a [\sigma_s^e N_2(r, \phi, z) - \sigma_s^a N_1(r, \phi, z)] \varphi_s(r, \phi) r dr d\phi \right\} \\ &\quad \times P_s^\pm(z) - \alpha_s P_s^\pm(z) \\ g(r, \phi, z) &= \sigma_s^e N_2(r, \phi, z) - \sigma_s^a N_1(r, \phi, z) \end{aligned}$$

Where index  $P$  and  $S$  stand for pump wave and signal wave respectively, + and - correspond to forward and backward propagation waves respectively,  $\sigma_a$  and  $\sigma_e$  are the corresponding absorption and emission cross section,  $N_1$  and  $N_2$  represent the numbers of Yb-ions in ground state and excited state,  $\varphi$  is the overlap factor,  $\lambda$  is the wavelength,  $\gamma$  is the nonlinear Kerr coefficient,  $\alpha$  is the loss coefficient,  $\tau$  is the life of the excited state population. For different pump configuration, the gain distribution  $g(r, \phi, z)$  of amplifier is different, which leads to the difference of HOM distribution along the fiber.

With the theoretical model, the HOM distribution caused by MI along the active fiber has been simulated for the fiber amplifier with different pumping configurations, as shown in Figure 7. When the power ratio of HOM exceeded 5%, the MI threshold was reached, and the power ratio of HOM would increase along the active fiber for both forward and backward pump configurations. However, compared with the backward pump scheme, the MI-induced HOMs was closer to the input end for the forward-pump schemes, as Figure 7 illustrated. Therefore, for forward pumped PM fiber amplifier, due to the fiber coiling, the HOMs would leak into the cladding, and a small part of the cladding signal light was able to reinject into the active core during propagating along the fiber. The polarization state of the reinjected signal light was random due to the scramble of the cladding, and reinjected signal light was amplified by the Yb-ions and in the PM fiber amplifier, and the polarization state was maintained [36], leading to the degradation of the PER. For backward pump scheme, the HOMs was mainly generated at the output end, which resulted in that the leaking and reinjecting process happened in passive fiber. The small portion of the reinjected signal light cannot be amplified, thereby the PER showed no obvious degradation.

### 5 Conclusion

In conclusion, the impact of MI effect on PER of the backward pumped PM fiber amplifier have been investigated, which revealed that the MI effect had little impact on PER for backward pump PM fiber amplifier. Comparing the experimental results of forward pumped amplifiers, where the MI induced the decrease of PER, one can conclude that the different pump power distribution can

influence the leaking and reinjecting process of HOM, and then leading to the different results with different pump configuration. Therefore, to circumvent MI-induced polarization degradation, backward pumping configurations should be preferentially adopted in high-power PM fiber laser systems.

## Data availability statement

The original contributions presented in the study are included in the article/supplementary material, further inquiries can be directed to the corresponding author.

## Author contributions

QS: Data curation, Writing – review and editing, Writing – original draft, Investigation, Validation. CZ: Writing – review and editing, Data curation, Writing – original draft, Investigation, Conceptualization. FaL: Writing – original draft, Writing – review and editing, Formal Analysis, Investigation. QC: Supervision, Funding acquisition, Writing – original draft, Investigation, Writing – review and editing. CG: Investigation, Writing – review and editing, Writing – original draft, Formal Analysis. FeL: Investigation, Writing – review and editing, Writing – original draft, Formal Analysis. HZ: Writing – review and editing, Investigation, Writing – original draft, Formal Analysis. RT: Methodology, Conceptualization, Supervision, Writing – review and editing. HL: Writing – review and editing, Resources, Investigation, Project administration. JW: Writing – review and editing, Supervision, Project administration, Methodology, Resources.

## References

- Tröbs M, Barke S, Theeg T, Kracht D, Heinzel G, Danzmann K. Differential phase-noise properties of a ytterbium-doped fiber amplifier for the Laser Interferometer Space Antenna. *Opt Lett* (2010) 35(3):435–7. doi:10.1364/ol.35.000435
- Yang F, Ye Q, Pan Z, Chen D, Cai H, Qu R, et al. 100-mW linear polarization single-frequency all-fiber seed laser for coherent Doppler lidar application. *Opt Commun* (2012) 285(2):149–52. doi:10.1016/j.optcom.2011.09.030
- Diaz R, Chan SC, Liu JM. Lidar detection using a dual-frequency source. *Opt Lett* (2006) 31(24):3600–2. doi:10.1364/ol.31.003600
- Henderson A, Stafford R. Low threshold, singly-resonant CW OPO pumped by an all-fiber pump source. *Opt Express* (2006) 14(2):767–72. doi:10.1364/oe.14.000767
- Gapontsev V, Avdokhin A, Kadwani P, Samartsev I, Platonov N, Yagodkin R. SM green fiber laser operating in CW and QCW regimes and producing over 550 W of average output power. *Proc SPIE* (2014) 8964:896407. doi:10.1117/12.2058733
- Asha Dahiya S. Optimization of high frequency radio over fiber system using cascaded amplifier and dispersion compensation fiber. *J Opt* (2023) 52(3):1552–65. doi:10.1007/s12596-022-00988-9
- Asha Dahiya S. Large tunable 16-tupled millimeter wave generation utilizing optical carrier suppression with a tunable sideband suppression ratio. *Front Phys* (2021) 9:747030. doi:10.3389/fphy.2021.747030
- Liu Z, Ma P, Su R, Tao R, Ma Y, Wang X, et al. High-power coherent beam polarization combination of fiber lasers: progress and prospect [Invited]. *J Opt Soc Am B* (2017) 34:A7–A14. doi:10.1364/josab.34.0000a7
- Flores A, Ehrehreich T, Holten R, Anderson B, Dajani and Iyad. Multi-kW coherent combining of fiber lasers seeded with pseudo random phase modulated light. In: *Fiber lasers XIII: technology, systems, and applications* (2016).
- Zheng Y, Yang Y, Wang J, Hu M, Liu G, Zhao X, et al. 10.8 kW spectral beam combination of eight all-fiber superfluorescent sources and their dispersion compensation. *Opt Express* (2016) 24(11):12063–71. doi:10.1364/oe.24.012063
- Wang Y, Peng W, Liu H, Yang X, Yu H, Wang Y, et al. Linearly polarized fiber amplifier with narrow linewidth of 5 kW exhibiting a record output power and near-diffraction-limited beam quality. *Opt Lett* (2023). 48:2909–2912.
- Smith AV, Smith JJ. Mode instability in high power fiber amplifiers. *Opt Express* (2011) 19:10180–92. doi:10.1364/oe.19.010180
- Brar K, Savage-Leuchs M, Henrie J, Courtney S, Dille C, Afzal R, et al. Threshold power and fiber degradation induced modal instabilities in high power fiber amplifiers based on large mode area fibers. *Proc SPIE* (2014) 8961:89611R. doi:10.1117/12.2042261
- Haarlammer N, Vries O, Liem A, Klüner A, Peschel T, Schreiber T, et al. Build up and decay of mode instability in a high power fiber amplifier. *Opt Express* (2012) 20:13274–83. doi:10.1364/oe.20.013274
- Ke W, Wang X, Bao X, Shu X. Thermally induced mode distortion and its limit to power scaling of fiber lasers. *Opt Express* (2013) 21:14272–81. doi:10.1364/oe.21.014272
- Tao R, Ma P, Wang X, Zhou P, Liu Z. 1.3 kW monolithic linearly polarized single-mode master oscillator power amplifier and strategies for mitigating mode instabilities. *Chin Laser Press* (2015) 3:86–93. doi:10.1364/prj.3.000086
- Wang Y, Liu Q, Ma Y, Sun Y, Peng W, Ke W, et al. Research of the mode instability threshold in high power double cladding Yb-doped fiber amplifiers. *Annalen der Physik* (2017) 529(8):1600398. doi:10.1002/andp.201600398
- Meng DR, Lai WC, He XB, Ma P, Su R, Zhou P, et al. Kilowatt-level, mode-instability-free, all-fiber and polarization-maintained amplifier with spectral linewidth of 1.8 GHz. *Laser Phys* (2019) 29(3):035103. doi:10.1088/1555-6611/aafd24
- Chang Z, Wang YS, Sun YH, Peng W, Ke W, Ma Y, et al. 1.5 kW polarization-maintained Yb-doped amplifier with 13 GHz linewidth by suppressing the self-pulsing and stimulated Brillouin scattering. *Appl Opt* (2019) 58(23):6419–25. doi:10.1364/ao.58.006419
- Wang YS, Feng YJ, Ma Y, Chang Z, Peng W, Sun Y, et al. 2.5 kW narrow linewidth linearly polarized all-fiber MOPA with cascaded phase-modulation to suppress SBS induced self pulsing. *IEEE Photon J* (2020) 12(3):1–15. doi:10.1109/jphot.2020.2997935

## Funding

The author(s) declare that financial support was received for the research and/or publication of this article. This work was supported by the National Natural Science Foundation of China (NSFC) (62205317), and the Youth Talent Climbing Foundation of the Laser Fusion Research Center.

## Conflict of interest

The authors declare that the research was conducted in the absence of any commercial or financial relationships that could be construed as a potential conflict of interest.

## Generative AI statement

The author(s) declare that no Generative AI was used in the creation of this manuscript.

## Publisher's note

All claims expressed in this article are solely those of the authors and do not necessarily represent those of their affiliated organizations, or those of the publisher, the editors and the reviewers. Any product that may be evaluated in this article, or claim that may be made by its manufacturer, is not guaranteed or endorsed by the publisher.

21. Chu QH, Shu Q, Guo C, Zhang H, Tao R, Tao R, Lin H, et al. 3 kW polarization maintained fiber lasers with 10.6 GHz linewidth and near diffraction limited beam quality. *Proc. SPIE 12595, Advanced Fiber Laser Conference (AFL2022), 125952G* (2021) 33(12):123006. doi:10.1117/12.2671818
22. Wang YS, Peng WJ, Feng YJ, Wang J, Yang X, et al. Influence of injected signal polarization on SBS, SRS, spectral broadening, and self-pulsing properties in high-power fiber amplifier. *Laser Phys Lett* (2022) 19(8):085102. doi:10.1088/1612-202x/ac7eca
23. Wang YS, Peng WJ, Wang J. Output of 4 kW < 10 GHz narrow linewidth linear polarization near diffraction limit fiber laser[J]. *High Power Laser Part Beams* (2023) 35(8):089901. doi:10.11884/HPLPB202335.230213
24. Kim DJ, Koo J, Jun SW, Jeong H, Lee H, Lee JH, et al. A 2 kW, 8 GHz linewidth Yb-doped polarization-maintained fiber laser with quasi-flat-top pseudo random binary sequence phase modulation for SBS suppression. *Nanomaterials* (2023) 13(8):1329, doi:10.3390/nano13081329
25. Liu H, Feng YJ, Yang XB, Wang Y, Yu H, Wang J, Peng W. 3.2-kW 9.7-GHz polarization-maintaining narrow-linewidth all-fiber amplifier. *Curr Opt Photon* (2024) 8(1):65–71.
26. Tao R, Ma P, Wang X, Zhou P, Liu Z. Theoretical study of pump power distribution on modal instabilities in high power fiber amplifiers. *Laser Phys Lett* (2016) 14:025002. doi:10.1088/1612-202x/aa4f8e
27. Smith AV, Smith JJ. Increasing mode instability thresholds of fiber amplifiers by gain saturation. *Opt Express* (2013) 21(3):15168–82. doi:10.1364/oe.21.015168
28. Wang Y. Stimulated Raman scattering in high-power double-clad fiber lasers and power amplifiers. *Opt Eng* (2005) 44(11):114202. doi:10.1117/1.2128147
29. Jauregui C, Limpert J, Tünnermann A. Derivation of Raman threshold formulas for CW double-clad fiber amplifiers. *Opt Express* (2009) 17(10):8476–90. doi:10.1364/oe.17.008476
30. Liu A, Chen X, Li M, Wang J, Walton DT, Zenteno LA. Comprehensive modeling of single frequency fiber amplifiers for mitigating stimulated Brillouin scattering. *J Lightwave Technol* (2009) 27(13):2189–2198.
31. Zha C, Peng W, Wang X, Wang Y, Li T, Ma Y, et al. Self-pulsing in kilowatt level narrow-linewidth fiber amplifier with WNS phase-modulation. *Opt Express* (2017) 25(17):19740–51. doi:10.1364/oe.25.019740
32. Otto HJ, Stutzki F, Jansen F, Eidam T, Jauregui C, Limpert J, et al. Temporal dynamics of mode instabilities in high-power fiber lasers and amplifiers. *Opt Express* (2012) 30(14):15710–22. doi:10.1364/oe.20.015710
33. Johansen MM, Laurila M, Maack MD, Noordegraaf D, Jakobsen C, Alkeskjold TT, et al. Frequency resolved transverse mode instability in rod fiber amplifiers. *Opt Express* (2013) 21(19):21847–56. doi:10.1364/oe.21.021847
34. Tao R, Ma P, Wang X, Zhou P, Liu Z. Experimental study on mode instabilities in all-fiberized high-power fiber amplifiers. *Chin Opt. Lett.* (2014) 12:S20603. doi:10.3788/col201412.s20603
35. Ward BG. Mode instability in coiled fiber amplifiers. *Proc SPIE Fiber Lasers XVII: Technology and Systems* (2020) 11260:1126016. doi:10.1117/12.2541977
36. Jauregui C, Kholaf S, Tu Y, Limpert J. Static modal energy transfer in high power, polarization maintaining fiber laser systems. *Proc SPIE Fiber Lasers XIX: Technology and Systems* (2022) 11981:1198110. doi:10.1117/12.2608224